



Article

Viticultural Suitability Analysis Based on Multi-Source Data Highlights Climate-Change-Induced Decrease in Potential Suitable Areas: A Case Analysis in Ningxia, China

Huiqing Bai ¹, Zhongxiang Sun ^{2,3}, Xuenan Yao ^{1,4}, Junhua Kong ¹, Yongjian Wang ¹ , Xiaoyu Zhang ⁵, Weiping Chen ⁶, Peige Fan ¹, Shaohua Li ¹, Zhenchang Liang ¹ and Zhanwu Dai ^{1,4,*}

- ¹ Beijing Key Laboratory of Grape Science and Enology and Key Laboratory of Plant Resources, Institute of Botany, The Chinese Academy of Sciences, Beijing 100093, China; huiqing.bai@ibcas.ac.cn (H.B.); xnyao@ibcas.ac.cn (X.Y.); kongjunhua@ibcas.ac.cn (J.K.); yongjian.wang@ibcas.ac.cn (Y.W.); fanpg@ibcas.ac.cn (P.F.); shhli@ibcas.ac.cn (S.L.); zl249@ibcas.ac.cn (Z.L.)
- ² China Agriculture Museum, Beijing 100125, China; sunzx@aircas.ac.cn
- ³ State Key Laboratory of Remote Sensing Science, Aerospace Information Research Institute, Chinese Academy of Sciences, Beijing 100094, China
- ⁴ University of Chinese Academy of Sciences, Beijing 100049, China
- ⁵ Key Laboratory for Meteorological Disaster Monitoring and Early Warning and Risk Management of Characteristic Agriculture in Arid Regions, China Meteorological Administration, Yinchuan 750002, China; zhang_xynet@163.com
- ⁶ Ningxia Horticulture Research Institute, Ningxia Academy of Agricultural and Forestry Sciences, Yinchuan 750002, China; nature06chen@163.com
- * Correspondence: zhanwu.dai@ibcas.ac.cn



Citation: Bai, H.; Sun, Z.; Yao, X.; Kong, J.; Wang, Y.; Zhang, X.; Chen, W.; Fan, P.; Li, S.; Liang, Z.; et al. Viticultural Suitability Analysis Based on Multi-Source Data Highlights Climate-Change-Induced Decrease in Potential Suitable Areas: A Case Analysis in Ningxia, China. *Remote Sens.* **2022**, *14*, 3717. <https://doi.org/10.3390/rs14153717>

Academic Editor: Aaron Moody

Received: 30 May 2022

Accepted: 1 August 2022

Published: 3 August 2022

Publisher's Note: MDPI stays neutral with regard to jurisdictional claims in published maps and institutional affiliations.



Copyright: © 2022 by the authors. Licensee MDPI, Basel, Switzerland. This article is an open access article distributed under the terms and conditions of the Creative Commons Attribution (CC BY) license (<https://creativecommons.org/licenses/by/4.0/>).

Abstract: As a perennial plant with long productive span of 30–50 years, grapevine may experience cross-lifespan climate change, which can modify wine quality and challenge viticultural sustainability. Therefore, it is essential to evaluate the viticultural suitability by considering both current and future climate conditions. To this end, a maximum entropy model was proposed to delimitate potentially suitable areas for viticulture based on multi-source data in a novel wine region, Ningxia, China, considering both current and future climate conditions. Firstly, we combined traditional data of climate, soil, and topography with remote sensing data to screen predictors that best characterize current geographical distribution of vineyards. Then, we used those predictors to assess current suitability (2001–2020) in Ningxia. The results indicated altitude, aridity index during April–September (K0409), precipitation during July–September (P0709), normalized difference vegetation index during July–September (NDVI0709), soil organic carbon (SOC), and precipitation in September (P09) were key predictors to assess potential suitability for viticulture, and their threshold values ranged from 1075 m to 1648 m, 2.93 to 4.83, 103.1 mm to 164.1 mm, 0.1 to 0.89, 0.07 g/kg to 11 g/kg and 28.4 mm to 45.0 mm, respectively. Suitability maps revealed a total suitable area of 12029 km², among which the highly and moderately suitable areas accounted for 6.1% and 23.1%, respectively. Finally, the alteration in proportion of potential suitable areas due to changing climate was estimated. The potential suitable areas varied from 8742 km² to 10623 km² over the next 40 years (2022–2060) and decreased to 8826–9184 km² under a short-term sustainability (suitable only during current–2040). To further consider long-term and sustainable development of the wine industry (current–2060), total suitable areas dropped by 26.7–29.2% under different climate scenarios compared with current suitable areas (2001–2020). The conclusions provide indispensable guidance for vineyard zoning considering long-term climate change.

Keywords: grape; MaxEnt model; environment variables; suitability; climate change; remote sensing data

1. Introduction

The wine industry is known with huge market potential and high added value, and, therefore, is of importance in regional economic development [1]. At present, the wine industry has encountered a series of impacts from changing climate worldwide, which not only challenges sustainability of the wine industry in existing wine regions, but also opens opportunities for new regions [2–7]. To develop a sustainable wine industry in a novel region, identifying suitable viticulture zones is the critical step, because grapevine is a perennial plant with a long productive span of 30–50 years and may experience cross-lifespan climate change. Therefore, it is essential to evaluate the suitability of a viticulture zone considering both current and future climates, ensure a constant production of high-quality grapes and wines, and maintain a sustainable development of the wine industry.

Grape and wine quality is mainly determined by the “terroir”, which is made up of a series of factors, including climate, soil, cultivar, cultivation management, oenological techniques, cultural conventions, etc. [8,9]. Climate is the major factor influencing quantity and quality of grape and wine, such as yield, composition, aroma, and berry color [10]. Variable temperature regimes are necessary for each stage of grape growth [11]. For example, budbreak of grapevine requires a prolonged temperature above 10 °C, while the suitable temperature is over 15 °C during flowering [12,13]. Since temperature is the most critical factor [14], various bioclimatic indices have been proposed to explore climate suitability in order to mitigate the impacts of climate change, such as Winkler index (WI) [11] and growing season temperature (GST) [15]. Some researchers have applied these bioclimatic indices to classify viticultural suitability under current and future climate conditions across the world [16–21]. Moreover, multi-criteria climatic indices combining temperature and radiation factors have been proposed for viticulture zoning [22]. In addition, precipitation-related indicators have been used to categorize wine regions as well [23,24]. In particular, combining multiple indices for a better assessment of climatic suitability is crucial [5,10]. Overall, the above-mentioned studies indicate the suitability of wine regions has changed due to changing climate. In addition to climate factors, soil attributes are also essential for assessing viticultural suitability [25]. Soil provides nutrients and plentiful mineral elements for vines, affecting the composition of grape berries and wine characteristics (e.g., potassium concentrations and titratable acidity) [26,27]. Recently, soil variables combining traditional climate indices have been used to select the best predictors characterizing the vineyards to assess suitable areas in Spain, and the results confirmed that the compensated thermicity index and continentality index, as well as soil pH, clay content, capacity, and saturation humidity, are key factors impacting geographical distribution for all the cultivars studied [28]. Additionally, topography, such as altitude, aspect, and slope, indirectly affect grape growth through changing climate and soil conditions [13,29] and should be considered as a supplement to ecological suitability assessment of vineyards as well.

Previous research has evaluated viticultural suitability worldwide using different methodologies. One approach is to evaluate the ecological suitability based on selected environment indicators related to growth and development of grapevine [30–34]. The other approach is to establish a species distribution model combining the actual plantation of grapevine with its habitat variables [3,5,28,35,36], and the latter is more objective compared with the first, minimizing differences caused by diverse research scales [36]. As one of the commonly used species distribution models, the maximum entropy model (MaxEnt) based on the principle of maximum entropy [37] has low requirement on the quantity of existing sites and high prediction accuracy [38,39] and is widely used to predict potential suitable areas of species. However, only a few studies assessed the climatic [5,36,40] and ecological suitability [28,35] of wine grape based on MaxEnt model worldwide, mainly considering climate and soil factors. The remote sensing data has high precision in large-scale and long time series. Obviously, it is of great value to integrate remote sensing data with climate, soil, and topography data to more precisely estimate the ecological suitability in order to harvest high-quality grapes and produce premium wines.

As the sixth wine consumer in the world, China possesses huge potential in the wine industry [41]. Ningxia is the largest continuous wine grape plantation region, with the area of 380 km² by the end of 2019, accounting for 1/4 of the wine regions in China [42]. However, changing temperature continuously impacts wine production in China; for instance, the high-quality wine regions may decrease while warming temperature is favorable for planting late-maturing cultivars [43]. Therefore, it is of great significance to establish viticultural suitability with consideration of long-term sustainability. Currently, few studies on climatic [36] and ecological suitability [35] have been explored by using MaxEnt model in the wine regions of China under current climate conditions, mainly applying climate, soil, and topography data, let alone assessing the change in suitability under future climate. Meanwhile, MaxEnt model is currently the best ecological model for predicting the species distribution, and its prediction covers a larger area than other models, which is more consistent with actual occurrence data [44,45]. Since grapevine is a perennial plant with outstanding longevity, assessing ecological suitability of wine grape by integrating multi-source data is valuable to obtain high-precision results under both current and future climates.

Thus, this study, in a case study of Ningxia region of China, based on the geographical distribution of the vineyards collected, aimed to (i) apply MaxEnt model with multi-source data to accurately evaluate potential suitable areas of wine grape in Ningxia; (ii) explore threshold values of key environment variables affecting distribution of wine grape under the current climate; and (iii) highlight the potential suitable areas of wine grape by simultaneously considering both current and future climates in Ningxia.

2. Materials and Methods

2.1. Study Region and Vineyard Occurrence Record

Ningxia is a young wine region in China and the wine industry started about 30 years ago. Ningxia has typical continental climate and is located in the middle and upper Yellow River of northwest China, ranging from 35°14' to 39°23'N and from 104°17' to 107°39'E. The total annual sunshine hours are above 2000 h. The average temperature and total precipitation for grape growing season range from 12 °C to 21 °C and 160 mm to 400 mm. The diurnal temperature range of grape growing season is generally over 10 °C, fulfilling the requirements of high-quality grape production [46,47]. There are various topographies, including hill, plain, mountain, and tableland. The soil type is diverse, such as dark loessial soils, cultivated loessial soils, alluvial soils, grey-cinnamon soils, aeolian sandy soils, cumulated irrigated soils, etc. At present, a few white cultivars (Chardonnay, Riesling, and Vidal Blanc) and red cultivars (Cabernet Sauvignon, Cabernet Gernischt, Merlot, Cabernet Franc, Marselan, and Petit Verdot) are planted in Ningxia.

The geographic distribution data of 107 vineyards were collected in this study, stemming from National Geographic Information System for Grape Industry, related literature [48], and field survey. Data were supplemented and verified in combination with satellite map and GPS orientation (Figure 1). Finally, the information of planting sites, as well as corresponding longitude and latitude, were stored in CSV format.

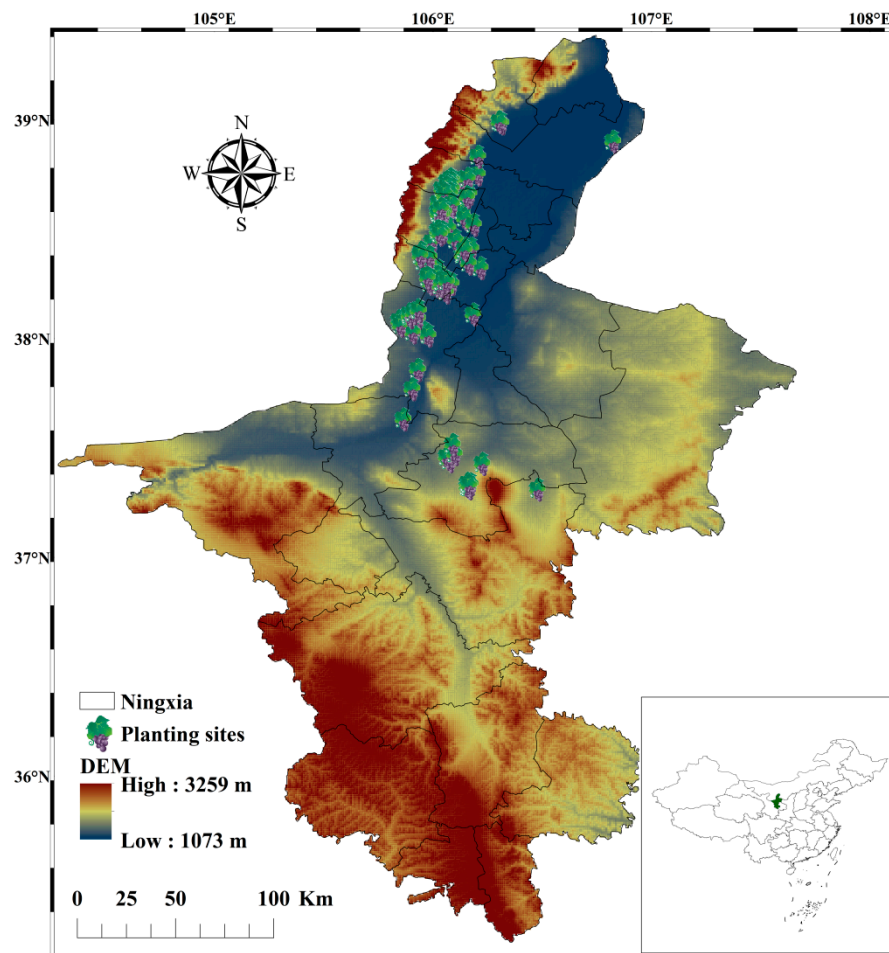


Figure 1. Study region and actual vineyard distribution in Ningxia (DEM = altitude).

2.2. Data Sources and Environment Variables

Environment variables were made up of four types of data in this research, including climate, soil, topography, and remote sensing. In terms of climate factors, air temperature derived from a reanalysis dataset named ERA5-Land [49] and precipitation applied an over 30-year quasi-global rainfall dataset named Climate Hazards Group InfraRed Precipitation with Station data (CHIRPS) [50]. These datasets were updated to present. The remote sensing data, such as land surface temperatures (LST) and normalized difference vegetation index (NDVI), stemmed from MODIS MOD11A2 V6 (<https://lpdaac.usgs.gov/products/mod11a2v006/>, accessed on 10 September 2021) and MOD13A2 V6 (<https://lpdaac.usgs.gov/products/mod13a2v006/>, accessed on 10 September 2021) products. Overall, climate and remote sensing data during 2001–2020 were downloaded from Google Earth Engine (<https://earthengine.google.com/>, accessed on 10 September 2021). Soil organic carbon is an extremely important component of soil and is closely related to soil fertility. The sand, silt, and clay contents were applied in the previous related research [28,35]; hence, soil texture, as the comprehensive factor of sand, silt, and clay contents, was chosen here. Furthermore, due to irrigation and fertilization in the wine region of Ningxia, soil retention capacity and soil nutrients (e.g., nitrogen, phosphorus and potassium) were not considered. Ultimately, soil organic carbon (0–5 cm), pH (0–5 cm), and texture (0–5 cm) were chosen and downloaded from SoilGrids (<https://www.soilgrids.org/>, accessed on 10 September 2021). In addition, altitude, namely DEM, was derived from the ASTER GDEM V3 data, and slope and aspect were calculated by altitude.

To discriminate effects of climate factors during different grape growth stages, grape growth was divided into four phenological stages from April to September in Ningxia, i.e., budburst (April), flowering (May and June), veraison (July and August), and maturity

(September). The habitat factors of the four stages were calculated accordingly. In addition, the average temperature in January, as a vital climatic index, was added to represent the dormant period of grapevine [13]. Since the solar radiation during grape growing season is not a limiting factor in Ningxia, it was unconsidered [46]. Furthermore, the aridity index (K) was applied instead of dryness index (DI), calculated by crop coefficient due to indistinct values of crop coefficient in different subregions of Ningxia [46]. Ultimately, 28 environment variables were applied to develop the MaxEnt model and assess potential suitable areas for wine grape in Ningxia (Table 1). It is noteworthy that the downloaded 28 environment variables in TIF format were converted to ASCII format by ArcGIS and kept at the same resolution (1 km × 1 km) as LST and NDVI.

Table 1. Definition of environment variables.

Environment Variables	Abbreviation	Resolution	Units
Average atmospheric temperature in January	TEM01	10 km	°C
Average atmospheric temperature in April	TEM0409	10 km	°C
Average atmospheric temperature from May to June	TEM0506	10 km	°C
Average atmospheric temperature from July to August	TEM0708	10 km	°C
Average atmospheric temperature in September	TEM09	10 km	°C
Average surface temperature in January	LST01	1 km	°C
Average surface temperature from April to September	LST0409	1 km	°C
Average surface temperature from May to June	LST0506	1 km	°C
Average surface temperature from July to August	LST0708	1 km	°C
Average surface temperature from July to September	LST0709	1 km	°C
NDVI from April to September	NDVI0409	1 km	
NDVI from May to June	NDVI0506	1 km	
NDVI from July to August	NDVI0708	1 km	
NDVI from July to September	NDVI0709	1 km	
NDVI in September	NDVI09	1 km	
Dryness from July to September	K0709	10 km	
Dryness from April to September	K0409	10 km	
Total precipitation from April to September	P0409	5 km	mm
Total precipitation from May to June	P0506	5 km	mm
Total precipitation from July to August	P0708	5 km	mm
Total precipitation from July to September	P0709	5 km	mm
Total precipitation in September	P09	5 km	mm
Soil organic carbon	SOC	250 m	g/kg
Soil pH	pH	250 m	
Soil texture	ST	250 m	
Altitude	DEM	30 m	m
Aspect	AS	30 m	
Slope	SL	30 m	degree

2.3. MaxEnt Setting and Modeling

MaxEnt is based on the principle of maximum entropy by using a machine-learning algorithm to predict potential suitability of species from presence-only data and habitat factors [35]. MaxEnt performs well in modeling species niches, even though there are limited occurrence data [51]. Here, MaxEnt version 3.4.1 downloaded from the American Museum of Natural History (biodiversityinformatics.amnh.org/open_source/maxent, accessed on 1 September 2021) was applied to assess potential suitable areas of wine grape in Ningxia. Seventy-five percent of sample data were randomly selected as a training set for prediction, while the remaining 25% of records were used as a test set to verify accuracy of this model [52]. In order to reduce randomness of the model and uncertainty of simulated results, the model was run repeatedly for 10 replicates [53]. The number of iterations and convergence threshold were set to 5000 and 10^{-5} , which allows the model to have adequate time for convergence. Finally, the training would stop if the log loss per iteration dropped below them [37]. The output format chosen was logistic, which represented the probability

of existence (ranging between 0 and 1) [54]. All other parameters were set to their default values. Additionally, the jackknife test was selected to determine dominant variables that affected the distribution of wine grape.

To evaluate the accuracy of simulated results by MaxEnt model, the training areas under the receiver operating characteristic (ROC) curve, namely AUC, was applied. AUC is a threshold independent measure of model performance, ranging from 0 to 1 [55]. The overall accuracy of the developed model was divided into excellent ($AUC > 0.9$), good ($0.8 < AUC \leq 0.9$), fair ($0.7 < AUC \leq 0.8$), poor ($0.6 < AUC \leq 0.7$), and fail ($AUC \leq 0.6$) [56]. The true skill statistic (TSS) with the formula of “sensitivity + specificity – 1” was applied to validate the performance of MaxEnt model as well, ranging from –1 to 1. Moreover, the closer the value was to 1, the better the model performed [57]. Based on previous studies, grape suitability was divided into highly suitable areas ($p \geq 0.66$), moderately suitable areas ($0.33 \leq p < 0.66$), lowly suitable areas ($0.05 \leq p < 0.33$), and unsuitable areas ($p < 0.05$) [36,58].

2.4. Future Climate Scenarios

Future temperature and precipitation data were derived from Coupled Model Inter-comparison Phase 6 (CMIP6) and downloaded from the WorldClim global climate dataset on a 2.5 arc-minute grid (<https://worldclim.org/>, accessed on 8 November 2021). Here, we selected a global climate model (GCM) named BCC-CSM2-MR from National Climate Center of China and four Shared Socio-Economic Pathways (SSPs: SSP126, SSP245, SSP370, and SSP585) to assess the suitability of wine grape in Ningxia for the periods of 2022–2040 and 2041–2060. Thereinto, SSP126, as the lowest radiation emission scenario, has a radiative forcing of 2.6 W m^{-2} with global warming below $2 \text{ }^\circ\text{C}$ until 2100. SSP245 and SSP370 are under a radiative forcing of 4.5 W m^{-2} and 7.0 W m^{-2} , and SSP585 represents the highest radiation emission scenario, with a radiative forcing of 8.5 W m^{-2} [59–61]. Firstly, the monthly average minimum, maximum temperature, and monthly total precipitation (12 bands from January to December in each variable) were downloaded under four scenarios for the periods of 2022–2040 and 2041–2060 in Ningxia. Then, the K0409 and P0709 during 2022–2060 were calculated by average temperature and total precipitation of April–September, as well as total precipitation during July–September by merging multi-band of ArcGIS software. Finally, since NDVI0709 under future climate conditions is not available, K0409, P09, and P0709 during 2022–2060 combined with DEM, SOC, and NDVI0709 across 2001–2020 were used to assess the viticultural suitability in order to analyze the change in areas caused by only changing climate (temperature and precipitation) (Figure 2).

2.5. Data Analysis

The environment variables of the same category may be correlated with each other, reducing predicted accuracy of the model [61]. The “Corrplot” package in R was used to analyze the correlation of selected environment variables in R 3.4.4 (developed by R Core Team and downloaded from Vienna, Austria) [62]. The threshold value for the Pearson correlation coefficient was set as 0.9, and environment variables with high correlation were divided into different combinations to minimize autocorrelation. Firstly, we used 28 environment variables to develop MaxEnt model and determined the percent contribution and permutation importance of each variable. The results showed that the percent contribution of DEM and K0409 were high and the percent contribution of TEM0709, TEM0409, NDVI0409, NDVI0709, LST0409, and LST0709 were low. Therefore, we deleted P0409, P0708, and K0709 (high correlation with DEM and K0409), as well as TEM0709, TEM0409, NDVI0409, NDVI0506, LST0409, and LST0709 (low percent contribution). Secondly, due to the high correlation among TEM0708, TEM0506, NDVI0709, NDVI0708, LST0708, and LST0506, we separated those highly correlated variables and combined them with TEM01, LST01, K0409, SL, AS, DEM, ST, pH, SOC, P09, P0506, and P0709. Finally, 10 combinations of environment variables were set (Table 2), and the dominant variables used for modeling were chosen from the optimal combination.

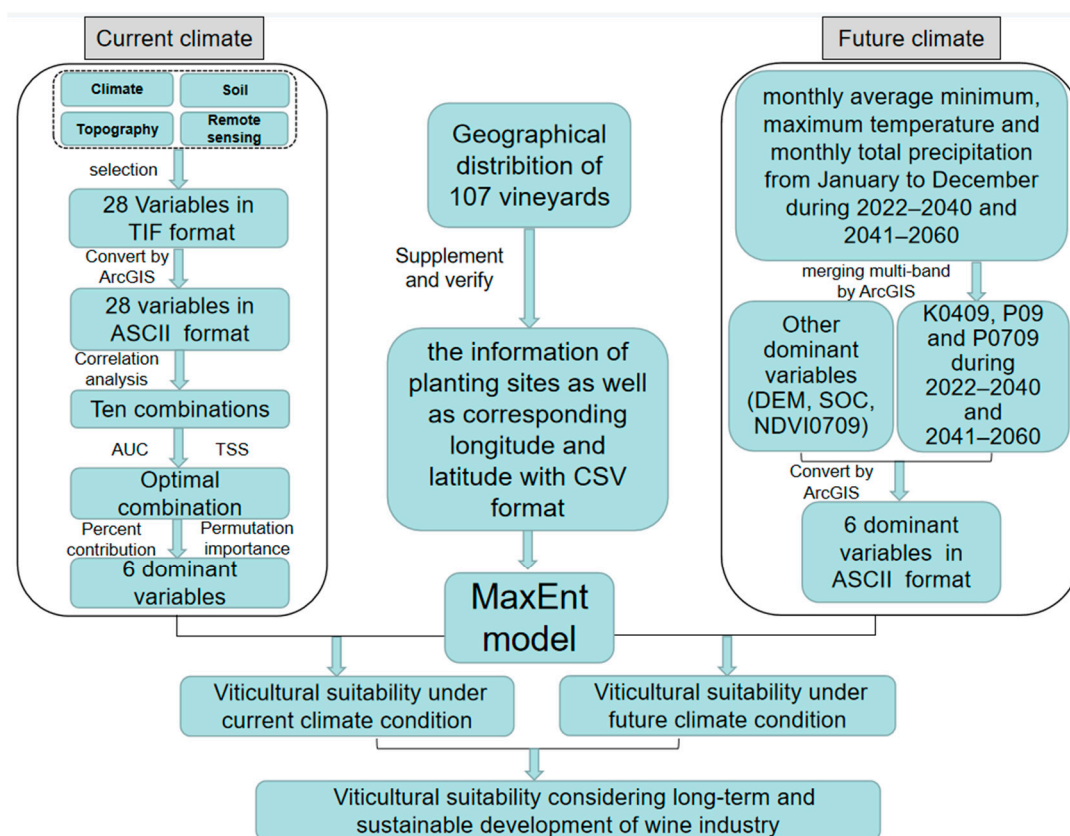


Figure 2. The workflow from data transformation to simulation of MaxEnt model under current and future climate conditions.

Table 2. Ten combinations of environment variables.

Group	Environment Variable Combination
G1	TEM01, TEM0506, P0506, P09, P0709, K0409, ST, pH, SOC, DEM, SL, AS, LST01, LST0708
G2	TEM01, TEM0708, P0506, P09, P0709, K0409, ST, pH, SOC, DEM, SL, AS, LST01, LST0708
G3	TEM01, TEM0506, P0506, P09, P0709, K0409, ST, pH, SOC, DEM, SL, AS, LST01, NDVI0708
G4	TEM01, TEM0506, P0506, P09, P0709, K0409, ST, pH, SOC, DEM, SL, AS, LST01, NDVI0709
G5	TEM01, TEM0708, P0506, P09, P0709, K0409, ST, pH, SOC, DEM, SL, AS, LST01, NDVI0708
G6	TEM01, TEM0708, P0506, P09, P0709, K0409, ST, pH, SOC, DEM, SL, AS, LST01, NDVI0709
G7	TEM01, TEM0506, P0506, P09, P0709, K0409, ST, pH, SOC, DEM, SL, AS, LST01, LST0506, NDVI0708
G8	TEM01, TEM0506, P0506, P09, P0709, K0409, ST, pH, SOC, DEM, SL, AS, LST01, LST0506, NDVI0709
G9	TEM01, TEM0708, P0506, P09, P0709, K0409, ST, pH, SOC, DEM, SL, AS, LST01, LST0506, NDVI0708
G10	TEM01, TEM0708, P0506, P09, P0709, K0409, ST, pH, SOC, DEM, SL, AS, LST01, LST0506, NDVI0709

In addition, the percent contribution represents the contribution of environment variables in the MaxEnt model. The higher the percent contribution is, the greater the contribution of the environment variable. The permutation importance represents the dependence of model on environment variables. The higher the permutation importance is, the greater the dependence [54]. Generally, the optimal combination and the key variables from the optimal combination were selected and the threshold of percent contribution was set as 5%.

3. Results

3.1. Accuracy of Maxent Model

The AUC values of training and test datasets were both over 0.9 for 10 combinations (Table 3). Among them, G10 (TEM01, TEM0708, P0506, P09, P0709, K0409, ST, pH, SOC, DEM, SL, AS, LST01, LST0506, and NDVI0709) performed the highest AUC values, with 0.984

and 0.979, respectively (Table 3). Moreover, the correlation coefficient for each environment variable of G10 was lower than 0.9, minimizing autocorrelation impacts on MaxEnt model accuracy (Figure 3). All the TSS values were over 0.80, indicating that the performance of each model was good. Overall, the simulated results were highly accurate, indicating that the model could be used to predict the potential suitability of wine grape in Ningxia.

Table 3. The areas under the receiver operating characteristic curve (AUC) and true skill statistic (TSS) values of MaxEnt model under 12 combinations of environment variables.

Environment Variable Combination	Training AUC	Test AUC	Training TSS	Test TSS
G1	0.982	0.974	0.875	0.872
G2	0.982	0.978	0.871	0.881
G3	0.983	0.975	0.868	0.858
G4	0.983	0.977	0.855	0.860
G5	0.982	0.973	0.854	0.859
G6	0.983	0.970	0.871	0.873
G7	0.983	0.978	0.820	0.872
G8	0.984	0.976	0.869	0.858
G9	0.984	0.978	0.855	0.864
G10	0.984	0.979	0.857	0.864
All (28 environment variables)	0.980	0.978	0.801	0.800
Six (6 dominant environment variables)	0.972	0.970	0.880	0.886

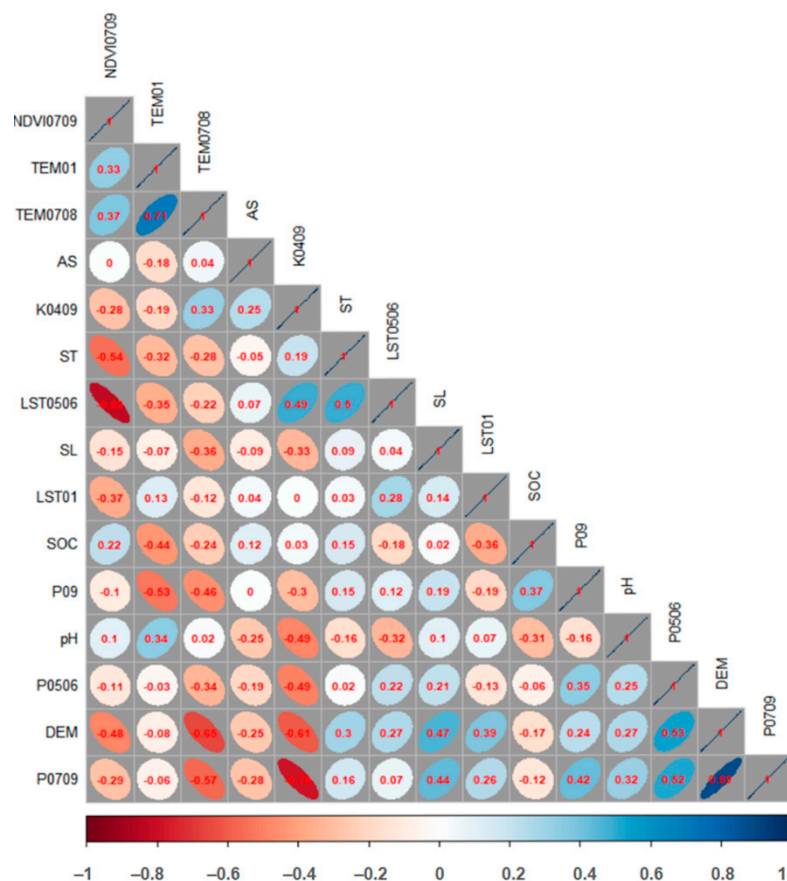


Figure 3. The correlation of each environment variable for optimal combination. Note: TEM01 and TEM0708 represent air temperature in January and from July to August. LST0506 and LST01 represent land surface temperature from May to June and in January. DEM, AS, and SL represent altitude, aspect, and slope. K0409 represents aridity index from April to September. P0709 and P09 represent total precipitation from July to September and in September. ST and SOC represent soil texture and soil organic carbon. NDVI0709 represents NDVI from July to September.

3.2. Dominant Environment Variables Impacting Wine Grape Distribution

Based on the analysis of percent contribution, the contributions of DEM, K0409, P0709, NDVI0709, SOC, and P09 were all over 5% (Figure 4a). DEM possessed the highest percent contribution, with the value of 32%. In terms of climate variables, the percent contributions of K0409, P0709, and P09 were 22.5%, 7.8%, and 6.4%, respectively. For remote sensing and soil variables, the percent contributions of NDVI and SOC were 7.4% and 6.5%, respectively. Additionally, permutation importance represented the importance of an individual variable in the model, and the permutation importance of P0709, DEM, and P0506 were above 20%, as detailed in Figure 3a. However, the percent contribution of P0506 was 1%, even with higher permutation importance. Irrigation is indispensable due to insufficient precipitation from May to June [47]; thus, the P0506 was unconsidered as a key factor affecting vineyard distribution. The results from jackknife test showed the similar performance with percent contribution (Figure 4b). DEM and K0409 had the maximum AUC value when they were used in isolation, highlighting their importance in determining model accuracy. Additionally, the AUC values of P09, P0709, SOC, and NDVI0709 were above 0.6. Eventually, the DEM, K0409, P0709, NDVI0709, SOC, and P09 were selected to assess potential suitable areas for wine grape in Ningxia. The mean AUC value of MaxEnt model based on six variables was 0.971, which demonstrated that this model has excellent predictive ability to describe the distribution of wine grape in Ningxia.

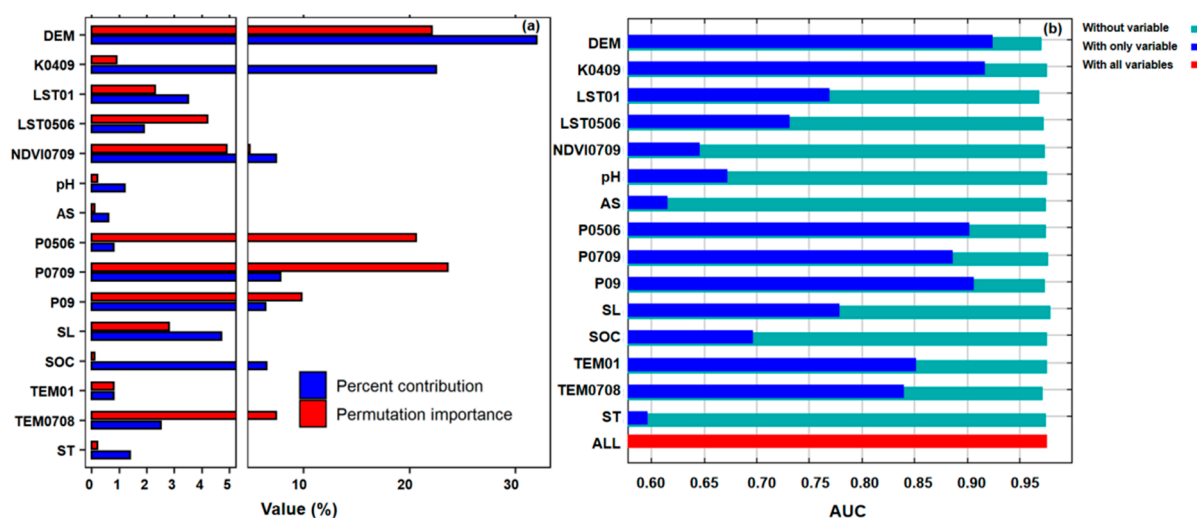


Figure 4. The percent contribution and permutation importance of each environment variable (a) and AUC values of each environment variable from the jackknife test (b). “With all variables” represents the AUC of the model using all variables, “With only variable” represents the AUC of the model using only one variable, and “Without variable” represents the AUC of the model using all except one variable.

3.3. Threshold Values of Six Dominant Environment Variables

In order to profoundly understand the relationships between distribution of wine grape and environment variables, the thresholds of six main variables were calculated. The values for DEM indicated that wine grapes are suitable for low and middle altitude, ranging from 1075 m to 1648 m in Ningxia (Figure 5a). In terms of climate variables, the thresholds of K0409, P09, and P0709 in the whole suitable areas ($p > 0.05$) were from 2.93 to 4.83, 28.4 mm to 45.0 mm, and 103.1 mm to 164.1 mm, respectively (Figure 5b–d). NDVI0709 represented the average vigor of plant growth from July to September; its threshold ranged from 0.1 to 0.89 (Figure 5e). The threshold of SOC ranged from 0.07 g/kg to 11 g/kg, which suggested large differences in terroir among different sub-regions in Ningxia (Figure 5f).

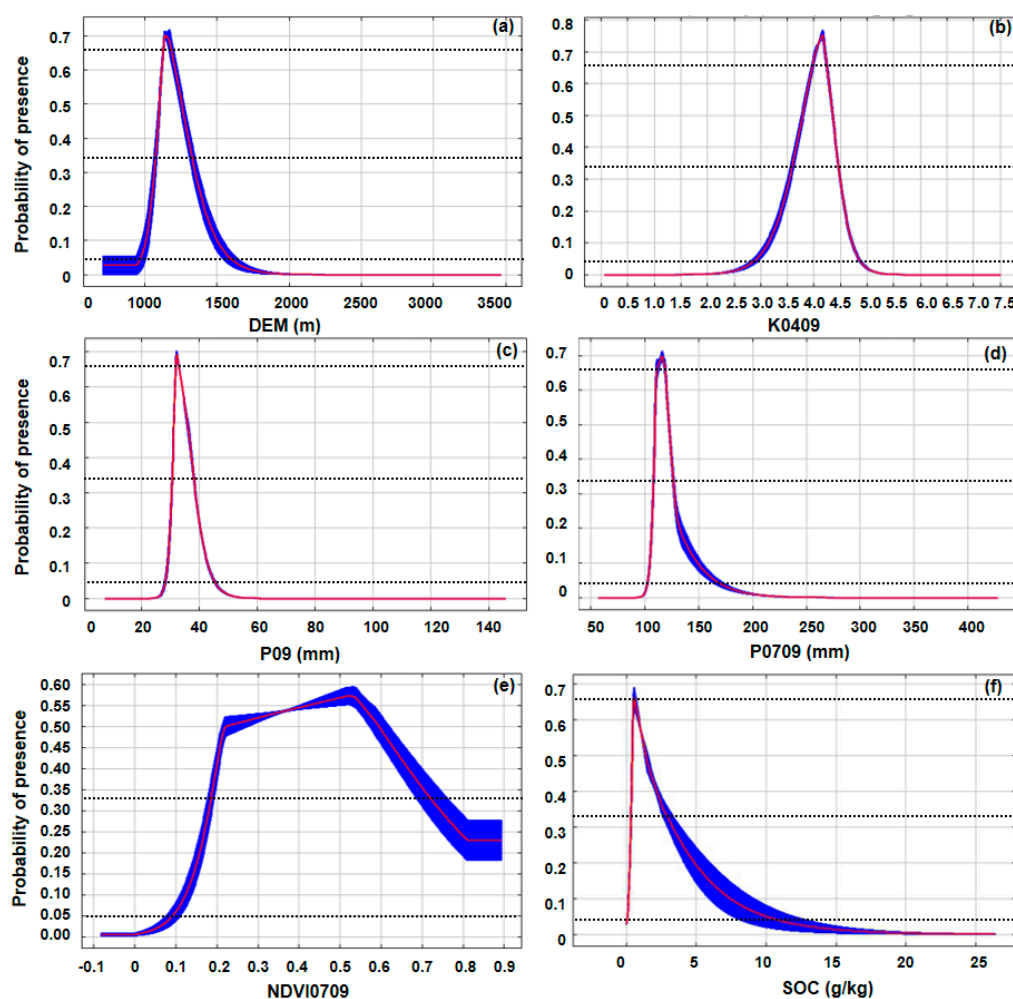


Figure 5. Response curves of dominant environment variables (DEM (a), K0409 (b), P09 (c), P0709 (d), NDVI0709 (e), SOC (f)) in the MaxEnt model. Note: response curves showed the relationships between existence probability of wine grape and six environment variables. Blue line represents the standard deviation (SD) of 10 replicates and red line represents mean value. DEM represents altitude. K0409 represents aridity index from April to September. NDVI0709 represents NDVI from July to September. P0709 and P09 represent total precipitation from July to September and in September. SOC represents soil organic carbon.

3.4. Potential Suitable Areas for Wine Grape under Current Climate Condition

Predicted results based on six dominant environment variables fitted well to the known wine regions in Ningxia under the current climate (Figure 6). The total suitable areas were 12,029 km², which accounted for 18.1% of the whole areas of Ningxia, and highly and moderately suitable areas accounted for 6.1% and 23.1% among the total suitable areas, respectively. The potential suitable areas were distributed in the north of Ningxia. Thereinto, highly suitable areas were mainly distributed in Xixia, Qingtongxia, Helan, and Yongning, a small amount in Xingqing, Lingwu, and Jinfeng, and scattered throughout in Pingluo, Dawukou, and Litong. The values of DEM, K0409, P09, and P0709 were below 1100 m, 4.1–4.2, below 35 mm, and below 120 mm, respectively, in highly suitable areas. Moderately suitable areas were mainly distributed in Qingtongxia, Helan, Yongning, Lingwu, Dawukou, Xingqing, Jinfeng, Xixia, and Litong, a small amount in Huinong and Pingluo, and scattered throughout in Shapotou and Zhongning. The values of DEM, K0409, P09, and P0709 were 1100–1200 m, above 3.9, below 40 mm, and below 130 mm, respectively, in moderately suitable areas. The distribution of low suitability was similar with both high and moderate suitability and distributed in Hongsipu, Yanchi, and Tongxin as well (Figure 6).

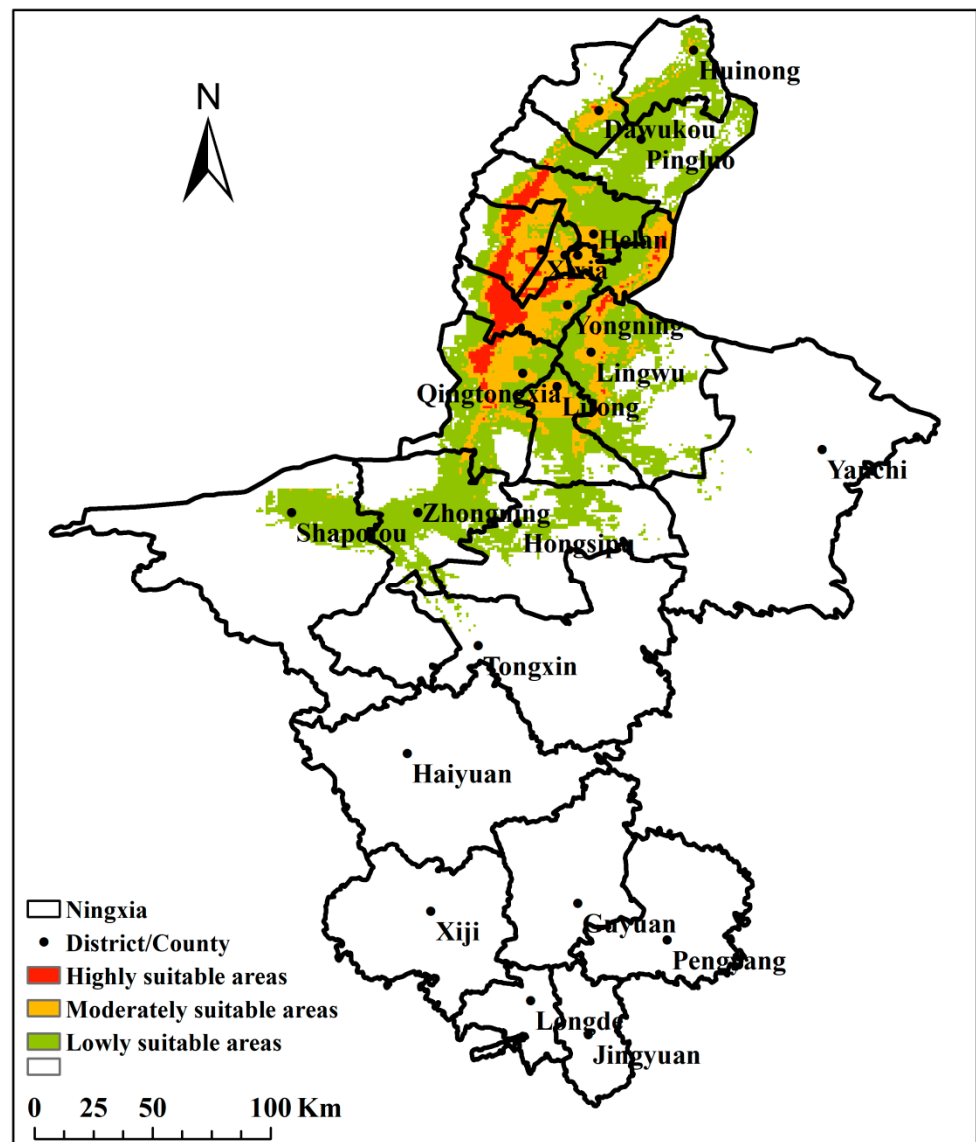


Figure 6. The potential suitable areas for wine grape under current climate in Ningxia.

3.5. Potential Suitable Areas for Wine Grape in Long-Term Climate Change

The simulations of potential suitable areas during 2001–2060 are encapsulated in Figure 7 and Table 4. The potential suitable areas ranged from 8826 km² to 9184 km² under a short-term sustainability (suitable only from the current period to 2040) and decreased by 23.7–26.6% compared with the current potential suitable areas (2001–2020). If only considering future climate, the potential suitable areas varied from 8742 km² to 10,623 km² over the next 38 years (2022–2060) and declined by 11.7–27.3% compared with the current potential suitable areas (2001–2020). Significantly, to further consider long-term and sustainable development of the wine industry (current–2060), total potential suitable areas dropped by 26.7–29.2% under four climate scenarios compared with the current potential suitable areas (2001–2020). Overall, potential suitable areas with short-term sustainability (current–2040) shifted to west under low emission scenarios (SSP126 and SSP245), while those areas shifted to west and north under high emission scenarios (SSP370 and SSP585). For a far sustainability (2041–2060), potential suitable areas shifted to west and east under four emission scenarios. In addition, highly, moderately, and lowly suitable areas decreased 22–296 km², 1128–1369 km², and –519–1727 km² among four emission scenarios of four periods (current–2060, current–2040, 2022–2060, and 2041–2060).

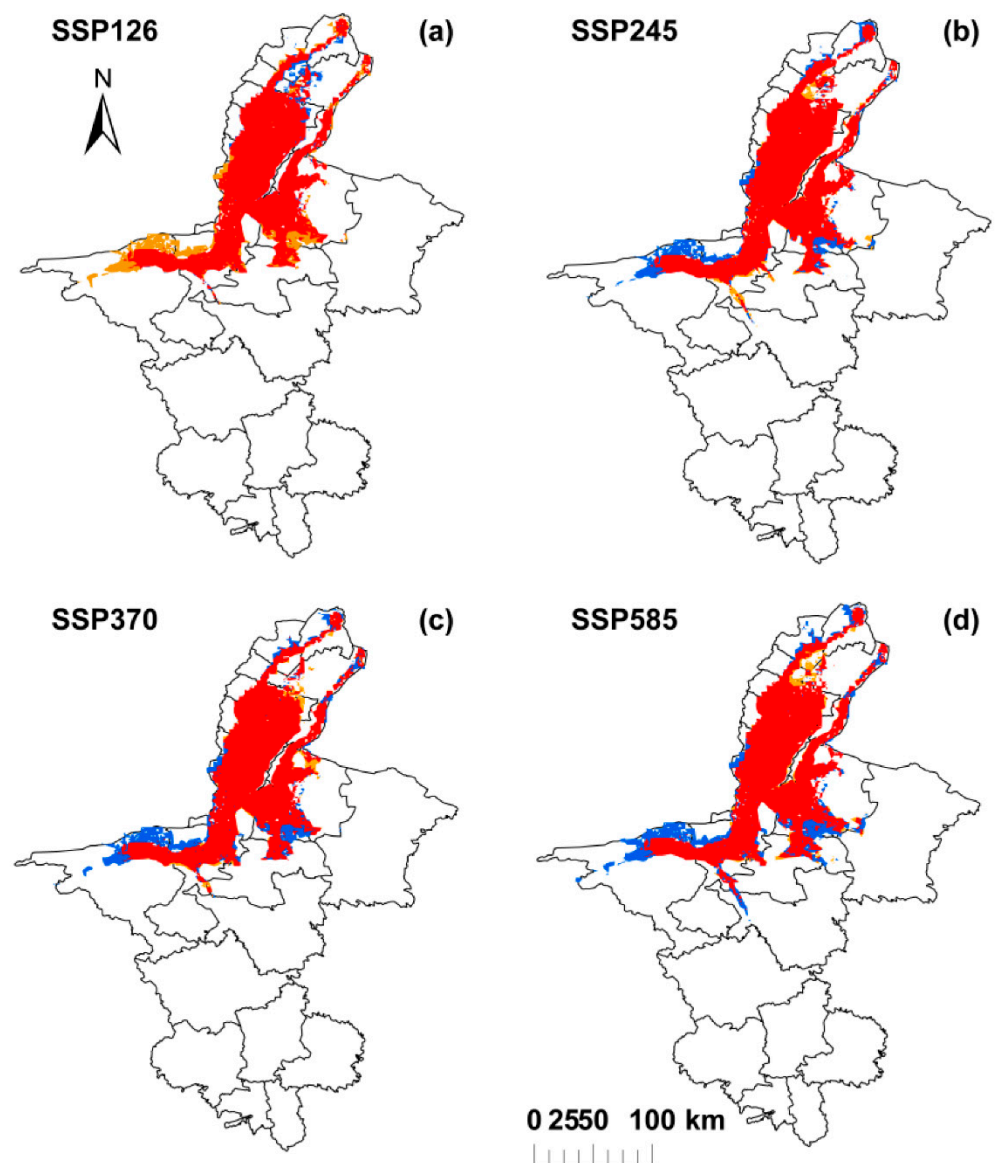


Figure 7. The potential suitable areas for wine grapes under SSP126 (a), SSP245 (b), SSP370 (c), and SSP585 (d) during the period of 2001–2060 in Ningxia. Red represents potential suitable areas of wine grape with long-term sustainability (current–2060). Orange represents potential suitable areas of wine grape with short-term sustainability (suitable only from current period to 2040). Blue represents new suitable areas of wine grape, which are not currently suitable but will be suitable over the next 38 years.

Table 4. The potential suitable areas for wine grape during four periods under four emission scenarios in Ningxia.

Climate Scenarios	Periods	Highly Suitable Areas (km ²)	Moderately Suitable Areas (km ²)	Lowly Suitable Areas (km ²)
SSP126	Long-term sustainability (current–2060)	386	1305	6824
	Short-term sustainability (current–2040)	400	1408	7018
	Future sustainability (2022–2060)	589	1462	7821
	Far sustainability (2041–2060)	682	1508	9044
SSP245	Long-term sustainability (current–2060)	334	1436	6889
	Short-term sustainability (current–2040)	374	1523	7151
	Future sustainability (2022–2060)	529	1562	7746
	Far sustainability (2041–2060)	673	1646	8263

Table 4. Cont.

Climate Scenarios	Periods	Highly Suitable Areas (km ²)	Moderately Suitable Areas (km ²)	Lowly Suitable Areas (km ²)
SSP370	Long-term sustainability (current–2060)	379	1339	6798
	Short-term sustainability (current–2040)	391	1434	7020
	Future sustainability (2022–2060)	591	1459	7819
	Far sustainability (2041–2060)	643	1574	8070
SSP585	Long-term sustainability (current–2060)	371	1363	7085
	Short-term sustainability (current–2040)	392	1496	7295
	Future sustainability (2022–2060)	618	1492	8444
	Far sustainability (2041–2060)	708	1528	8745

4. Discussion

Climate change massively affects potential suitability of viticulture; identifying potential suitable areas of wine grapes can provide a tangible upper limit for improving grape and wine quality to develop the wine industry [3,5]. Here, our results provided a full representation of the viticultural potential by developing an optimal MaxEnt model based on both occurrence data of wine grape and dominant environment variables under current and future climates in Ningxia, China.

Although several environment variables were chosen to assess the ecological suitability of wine grape, selected variables were mainly climatic factors [5,34,40], followed by soil and topography [28,33]. In this study, we combined the data of climate, soil, and topography and remote sensing data (NDVI and LST) and divided phenological stages of grapevines into four periods to precisely estimate potential suitable areas. The final results demonstrated that selected variables with high contribution were DEM, K0409, P0709, NDVI0709, SOC, and P09. Previous research has also indicated that altitude is a crucial habitat factor impacting suitability of grapevine [5,35]. Our result not only established the importance of DEM, but also quantified the threshold values of potential suitable areas, ranging from 1075 to 1648 m in Ningxia. As an indicator of dryness and humidity in some areas, K0409 has been used to explore climatic and ecological suitability of wine grape [36,46]. K0409 possesses 22.5% model contribution, and its threshold values of suitable areas varies from 2.93 to 4.83 in this study. It is well known that a moderate water stress is actually desirable, because water deficits to a moderate level can improve fruit composition and advance ripening [63]. Jiang et al. [64] suggested that precipitation should not exceed 50 mm during harvest in order to obtain high-quality grape. Similarly, our results highlighted that the threshold values of P09 and P0709 range from 28.4 mm to 45.0 mm and 103.1 mm to 164.1 mm in potential suitable areas of Ningxia. In addition, we quantified the threshold value of SOC ranging from 0.07 g/kg to 11 g/kg in potential suitable areas as well. Soil organic carbon (SOC) reflects the ability of sequestration of carbon, directly affecting the maintenance and improvement of soil fertility and, thus, is often recognized as an important index to evaluate soil fertility [65]. Cheng et al. [66] demonstrated differences in grape composition associated with soil water and organic carbon. Finally, NDVI is considered as another variable impacting the distribution of wine grape here. The threshold value of NDVI0709 ranged from 0.21 to 0.37 under higher potential suitable areas, which is helpful for monitoring wine regions by remote sensing technology. Overall, our conclusions not only highlighted the key climate variables, but also provide topography, soil, and remote sensing variables that affect grapevine distribution in Ningxia, China.

Subsequently, this research also revealed the total suitable areas with the value of 12,029 km²; thereinto, highly suitable areas were 734 km² and mainly distributed in Xixia District, Qingtongxia City, Helan, and Yongning Counties. Some suitable regions are consistent with current plantation in Ningxia [67]. The results provided support to develop new planting areas, which are potentially suitable but are not planted currently. Although previous studies mainly estimated potential suitable areas combining the MaxEnt model

with climate and soil variables in different wine regions of world [5,28,33,34], we applied traditional variables of climate, soil, and topography, as well as remote-sensing-related indices and divided climate and remote sensing data into four periods based on phenological stages to accurately confirm which phenological period mainly affects the distribution of wine grape. Since grapevines possess a long life span of 30–50 years, it is not sufficient to explore currently potential suitable areas of wine grapes under continuously changing climate. Previous research has claimed that some cool wine regions, such as the UK [68] and Canada [69], may benefit from global warming by becoming suitable areas for wine grape. Conversely, Roussillon in France [70] and Romania [31] may become too hot to continuously produce high-quality wines. Therefore, we assessed potential suitable areas of wine grape in the coming decades as well. Our predictions identified that total suitable areas reduced in the future compared to a baseline of 2001–2020. The decrease is caused by decreased P09 and K0409, as well as increased P0709 during 2022–2060 compared with the current climate (Figure 8). In other countries, the future climate will be beneficial for wine production in Scotland under high-end climate change [71], whereas there will be a negative influence in the wine regions of central and southern Spain under future climate [72]. In the whole of Europe, the suitable areas for wine grape will slightly decline for 2050 as well [5]. Overall, climate change brings both opportunities and challenges for the wine industry. In Ningxia, China, the potential suitable areas declined under global warming conditions when considering the long-term sustainability (current–2060).

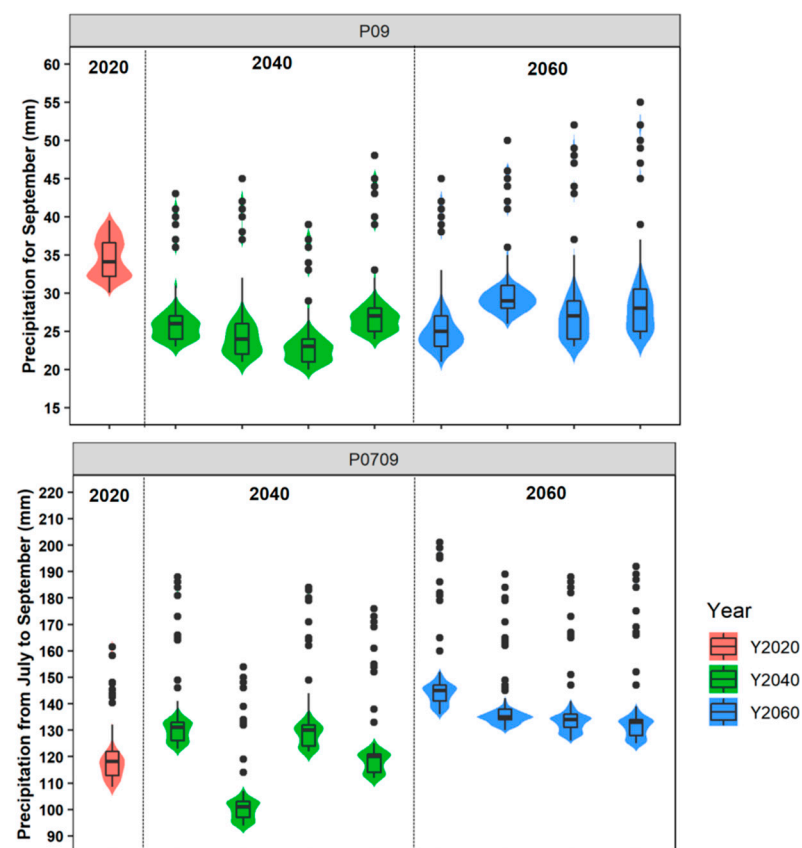


Figure 8. Cont.

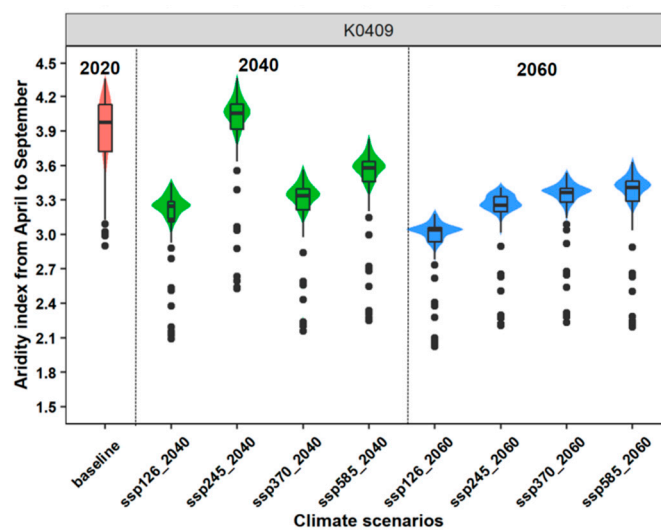


Figure 8. P09, P0709, and K0409 in Ningxia under current (2001–2020) and future (SSP126, SSP245, SSP370, and SSP585 for the periods of 2021–2060) climates. Note: P09, P0709, and K0409 represent total precipitation in September, total precipitation from July to September, and aridity index from April to September.

Each cultivar has its own optimal environment condition [28]; here, we did not consider the difference among cultivars. In the future, this key issue should be combined to evaluate potential suitable areas for each special cultivar. Moreover, climate change increases the intensity of some extreme weather events [73], such as extreme drought or spring frost; thus, those areas where extreme events are frequent should also be considered in future studies. In order to explore the changes in grapevine distribution from changing climate, we only changed climate factors and kept other factors constant under future climate scenario conditions. Despite all those limitations, our conclusions still highlight the different suitable areas under both current and future climate conditions. Those results can provide a guideline to develop new zones of viticulture and ensure low climate risks in the next several decades; meanwhile, it will further promote the sustainable development of the wine industry [3,5]. In the future research, assessing the potential suitability in the whole wine regions of China is indispensable based on multi-source data, accurate geographical distribution of grapes, multi-species distribution models, and multi-global climate models.

5. Conclusions

Overall, climate, soil, topography, and remote-sensing-related indices all exert important influences on the distribution of vineyards in Ningxia, namely, DEM, K0409, P0709, NDVI0709, SOC, and P09. We developed a MaxEnt model with these six habitat variables, which predicted the total potential suitable areas consistent with known wine regions in Ningxia. Moreover, these projections suggest that highly suitable areas are mainly distributed in Xixia, Qingtongxia, Helan, and Yongning, and moderately suitable areas are distributed in Dawukou, Xingqing, Jinfeng, Lingwu, and Litong as well. In addition, considering the sustainable development of the wine industry, the potential suitable areas decreased to 8826–9184 km² under a short-term sustainability (suitable only from the current period to 2040). Likewise, the potential suitable areas will decline over the next 38 years (2022–2060). To further consider long-term and sustainable development of the wine industry (current–2060), total potential suitable areas will drop by 26.7–29.2% compared with current potential suitable areas (2001–2020). These findings are helpful for delineating suitable adaptation strategies, providing insights into the challenges, and facilitating the long-term and sustainable development of wine regions in China.

Author Contributions: Z.D. and H.B. designed the study. H.B. wrote a first draft version of the manuscript. H.B. and X.Y. collected the vineyards. Z.S. provided the remote sensing data and suggested detailed improvements. All authors provided assistance in organizing and editing the manuscript. All authors have read and agreed to the published version of the manuscript.

Funding: This work was supported by the National Natural Science Foundation of China (U20A2041), National Key R&D Program of China (2021YFE0109500), and the Agricultural Breeding Project of Ningxia Hui Autonomous Region (NXNYYZ202101). The authors acknowledge the anonymous referees for their valuable comments.

Conflicts of Interest: The authors declare no conflict of interest.

References

1. Duchene, E. How can grapevine genetics contribute to the adaptation to climate change? *OENO One* **2016**, *50*, 113–124. [[CrossRef](#)]
2. Webb, L.B.; Whetton, P.H.; Barlow, E.W.R. Observed trends in winegrape maturity in Australia. *Glob. Chang. Biol.* **2011**, *17*, 2707–2719. [[CrossRef](#)]
3. Hannah, L.; Roehrdanz, P.R.; Ikegami, M.; Shepard, A.V.; Shaw, M.R.; Tabor, G.; Zhi, L.; Marquet, P.A.; Hijmans, R.J. Climate change, wine, and conservation. *Proc. Natl. Acad. Sci. USA* **2013**, *110*, 6907–6912. [[CrossRef](#)] [[PubMed](#)]
4. Fraga, H.; García de Cortázar Atauri, I.; Malheiro, A.C.; Santos, J.A. Modelling climate change impacts on viticultural yield, phenology and stress conditions in Europe. *Glob. Chang. Biol.* **2016**, *22*, 3774–3788. [[CrossRef](#)] [[PubMed](#)]
5. Tóth, J.P.; Végvári, Z. Future of winegrape growing regions in Europe. *Aust. J. Grape Wine Res.* **2016**, *24*, 64–72. [[CrossRef](#)]
6. Wolkovich, E.M.; de Cortazar-Atauri, I.G.; Morales-Castilla, I.; Nicholas, K.A.; Lacombe, T. From Pinot to Xinomavro in the world's future wine-growing regions. *Nat. Clim. Chang.* **2018**, *8*, 29–37. [[CrossRef](#)]
7. Morales-Castilla, I.; García de Cortázar-Atauri, I.; Cook, B.I.; Lacombe, T.; Parker, A.; van Leeuwen, C.; Nicholas, K.A.; Wolkovich, E.M. Diversity buffers wine growing regions from climate change losses. *Proc. Natl. Acad. Sci. USA* **2020**, *117*, 2864–2869. [[CrossRef](#)]
8. Van Leeuwen, C.; Gerard, S. The concept of terroir in viticulture. *J. Wine Res.* **2006**, *17*, 1–10. [[CrossRef](#)]
9. Van Leeuwen, C.; Friant, P.; Choné, X.; Tregoat, O.; Koundouras, S.; Dubourdieu, D. Influence of climate, soil, and cultivar on terroir. *Am. J. Enol. Vitic.* **2004**, *55*, 207–217.
10. Honorio, F.; García-Martín, A.; Moral, F.J.; Paniagua, L.L.; Rebollo, F.J. Spanish vineyard classification according to bioclimatic indexes. *Aust. J. Grape Wine Res.* **2018**, *24*, 335–344. [[CrossRef](#)]
11. Winkler, A.J.; Cook, J.A.; Kliever, W.M.; Lider, L.A. *General Viticulture*; University of California Press: Berkeley, CA, USA, 1974; pp. 58–70.
12. García de Cortázar-Atauri, I.; Brisson, N.; Gaudillere, J.P. Performance of several models for predicting budburst date of grapevine (*Vitis vinifera* L.). *Int. J. Biometeorol.* **2009**, *53*, 317–326. [[CrossRef](#)]
13. Zhang, C.T. *The Climatic Regionalization of Viticulture and Grapevine Variety Zoning over China*; Nanjing University of Information Science & Technology: Nanjing, China, 2012.
14. Fraga, H.; Pinto, J.G.; Santos, J.A. Climate change projections for chilling and heat forcing conditions in European vineyards and olive orchards: A multi-model assessment. *Clim. Chang.* **2019**, *152*, 179–193. [[CrossRef](#)]
15. Jones, G.V.; White, M.A.; Cooper, O.R.; Storchmann, K. Climate change and global wine quality. *Clim. Chang.* **2005**, *73*, 319–343. [[CrossRef](#)]
16. Hall, A.; Jones, G.V. Spatial analysis of climate in winegrape-growing regions in Australia. *Aust. J. Grape Wine Res.* **2010**, *16*, 389–404. [[CrossRef](#)]
17. Malheiro, A.C.; Santos, J.A.; Fraga, H.; Pinto, J.G. Climate change scenarios applied to viticultural zoning in Europe. *Clim. Res.* **2010**, *43*, 163–177. [[CrossRef](#)]
18. Neumann, P.; Matzarakis, A. Viticulture in southwest Germany under climate change conditions. *Clim. Res.* **2011**, *47*, 161–169. [[CrossRef](#)]
19. Ruml, M.; Vukovic, A.; Vujadinovic, M. On the use of regional climate models: Implications of climate change for viticulture in Serbia. *Agric. For. Meteorol.* **2012**, *158*, 53–62. [[CrossRef](#)]
20. Moriondo, M.; Jones, G.V.; Bois, B.; Dibari, C.; Ferrise, R.; Trombi, G.; Bindi, M. Projected shifts of wine regions in response to climate change. *Clim. Chang.* **2013**, *119*, 825–839. [[CrossRef](#)]
21. Fila, G.; Gardiman, M.; Belvini, P.; Meggio, F.; Pitacco, A. A comparison of different modelling solutions for studying grapevine phenology under present and future climate scenarios. *Agric. For. Meteorol.* **2014**, 195–196, 192–205. [[CrossRef](#)]
22. Huglin, P. Nouveau mode d'évaluation des possibilités héliothermiques d'un milieu viticole. *Comptes Rendus Séances L'académie D'agriculture Fr.* **1978**, *64*, 1117–1126.
23. Koufos, G.C.; Mavromatis, T.; Koundouras, S.; Jones, G.V. Response of viticulture-related climatic indices and zoning to historical and future climate conditions in Greece. *Int. J. Climatol.* **2017**, *38*, 2097–2111. [[CrossRef](#)]
24. Wang, J.; Zhang, X.; Su, L.; Li, H.; Zhang, L.; Wei, J. Global warming effects on climate zones for wine grape in Ningxia region, China. *Theor. Appl. Climatol.* **2020**, *140*, 1527–1536. [[CrossRef](#)]
25. White, R.E. The value of soil knowledge in understanding wine terroir. *Front. Plant Sci.* **2020**, *8*, 12. [[CrossRef](#)]

26. Jiménez-Ballesta, R.; Bravo, S.; Amoros, J.A.; Pérez-de-los-Reyes, C.; García-Pradas, J.; Sanchez, M.; García-Navarro, F.J. A morphological approach to evaluating the nature of vineyard soils in semiarid Mediterranean environment. *Eur. J. Soil Sci.* **2022**, *73*, e13201. [[CrossRef](#)]
27. Mackenzie, D.E.; Christy, A.G. The role of soil chemistry in wine grape quality and sustainable soil management in vineyards. *Water Sci. Technol.* **2005**, *51*, 27–37. [[CrossRef](#)] [[PubMed](#)]
28. Del Río, S.; Álvarez-Esteban, R.; Alonso-Redondo, R.; Hidalgo, C.; Penas, Á. A new integrated methodology for characterizing and assessing suitable areas for viticulture: A case study in Northwest Spain. *Eur. J. Agron.* **2021**, *131*, 126391. [[CrossRef](#)]
29. Strack, T.; Schmidt, D.; Stoll, M. Impact of steep slope management system and row orientation on canopy microclimate. Comparing terraces to downslope vineyards. *Agric. For. Meteorol.* **2021**, *307*, 108515. [[CrossRef](#)]
30. Moral, F.J.; Rebollo, F.J.; Paniagua, L.L.; García, A. Climatic spatial variability in Extremadura (Spain) based on viticultural bioclimatic indices. *Int. J. Biometeorol.* **2014**, *58*, 2139–2152. [[CrossRef](#)] [[PubMed](#)]
31. Irimia, L.M.; Patriche, C.V.; Quenol, H.; Sfică, L.; Foss, C. Shifts in climate suitability for wine production as a result of climate change in a temperate climate wine region of Romania. *Theor. Appl. Climatol.* **2017**, *131*, 1069–1081. [[CrossRef](#)]
32. Alsafadi, K.; Mohammed, S.; Habib, H.; Kiwan, S.; Hennawi, S.; Sharaf, M. An integration of bioclimatic, soil, and topographic indicators for viticulture suitability using multi-criteria evaluation: A case study in the Western slopes of Jabal Al Arab-Syria. *Geocarto Int.* **2020**, *35*, 1466–1488. [[CrossRef](#)]
33. Patriche, C.V.; Irimia, L.M. Mapping the impact of recent climate change on viticultural potential in Romania. *Theor. Appl. Climatol.* **2022**, *148*, 1035–1056. [[CrossRef](#)]
34. Skahill, B.; Berenguer, B.; Stoll, M. Temperature-based climate projections of Pinot noir suitability in the Willamette Valley American viticultural area. *OENO One* **2022**, *56*, 209–225. [[CrossRef](#)]
35. Lin, Z.Y.; Chen, Q.; Chen, C.Y.; Li, X.; He, P. Assessment of spatial distribution of Cabernet Sauvignon in Hengduanshan valley of western Sichuan based on MaxEnt model. *Chin. J. Agric. Resour. Reg. Plan.* **2020**, *4*, 144–155.
36. Wang, J.; Zhou, G.S. The climatic suitability and climatic impact factors affecting the wine grapes (*Vitis vinifera* L.) planting distribution in China. *Acta Ecol. Sin.* **2021**, *41*, 2418–2427.
37. Phillips, S.J.; Anderson, R.P.; Schapire, R.E. Maximum entropy modeling of species geographic distributions. *Ecol. Model.* **2006**, *190*, 231–259. [[CrossRef](#)]
38. Estes, L.D.; Bradley, B.A.; Beukes, H.; Hole, D.G.; Lau, M.; Oppenheimer, M.G.; Schulze, R.; Tadross, M.A.; Turner, W.R. Comparing mechanistic and empirical model projections of crop suitability and productivity: Implications for ecological forecasting. *Glob. Ecol. Biogeogr.* **2013**, *22*, 1007–1018. [[CrossRef](#)]
39. Guo, Y.L.; Zhao, Z.F.; Qiao, H.J.; Wang, R.; Wei, H.Y.; Wang, L.K.; Gu, W.; Li, X. Challenges and development trend of species distribution model. *Adv. Earth Sci.* **2020**, *35*, 1292–1305.
40. Callen, S.T.; Klein, L.L.; Miller, A.J. Climatic niche characterization of 13 North American *Vitis* species. *Aust. J. Grape Wine Res.* **2016**, *67*, 339–349. [[CrossRef](#)]
41. International Organisation of Vine and Wine (OIV). State of the World Vitivinicultural Sector in 2022. 2022. Available online: <https://www.oiv.int/public/medias/8778/eng-state-of-the-world-vine-and-wine-sector-april-2022-v6.pdf> (accessed on 1 May 2022).
42. Song, K.Y. Methods of enhancing economic benefits of wine industry in Ningxia. *Ningxia J. Agric. For. Sci. Technol.* **2020**, *61*, 60–62.
43. Zhang, Q.Z.; Tang, Y.H. Effects of climate change on wine grape production in China. *China Brew.* **2021**, *40*, 1–6.
44. Van Leeuwen, C.; Schultz, H.; Garcia de Cortazar-Atauri, I.; Duchêne, E.; Ollat, N.; Pieri, P.; Bois, B.; Goutouly, J.P.; Quénel, H.; Touzard, J.M.; et al. Why climate change will not dramatically decrease viticultural suitability in main wine producing areas by 2050. *Proc. Natl. Acad. Sci. USA* **2013**, *110*, E3051–E3052. [[CrossRef](#)] [[PubMed](#)]
45. Ma, M.X.; Zhang, H.; Gao, J.X.; Ju, C.H.; Wang, Y.S.; Liu, D.T. Different methods comparison of delineating the ecological protection red line for biodiversity conservation. *Acta Ecol. Sin.* **2019**, *39*, 6959–6965.
46. Zhang, X.Y.; Li, H.Y.; Chen, W.P.; Zhang, L.; Su, L.; Wang, J. Ecological regionalization of wine grape varieties in Ningxia. *Chin. J. Ecol.* **2014**, *33*, 3112–3119.
47. Serratos, M.P.; Marquez, A.; Lopez-Toledano, A.; Medina, M.; Merida, J. Changes in hydrophilic and lipophilic antioxidant activity in relation to their phenolic composition during the chamber drying of red grapes at a controlled temperature. *J. Agric. Food Chem.* **2011**, *59*, 1882–1892. [[CrossRef](#)]
48. Xie, X.L. *Study on Status of Wine Regions in China and Impact of Climate Change on It*; Northwest A&F University: Xianyang, China, 2018.
49. Muñoz Sabater, J. ERA5-Land Monthly Averaged Data from 1981 to Present. Copernicus Climate Change Service (C3S) Climate Data Store (CDS). 2019. Available online: <https://cds.climate.copernicus.eu/cdsapp#!/dataset/10.24381/cds.68d2bb30?tab=overview> (accessed on 10 September 2021).
50. Funk, C.; Peterson, P.; Landsfeld, M.; Pedreros, D.; Verdin, J.; Shukla, S.; Husak, G.; Rowland, J.; Harrison, L.; Hoell, A.; et al. The climate hazards infrared precipitation with stations—A new environmental record for monitoring extremes. *Sci. Data* **2015**, *2*, 150066. [[CrossRef](#)]
51. Zingore, K.M.; Sithole, G.; Abdel-Rahman, E.M.; Mohamed, S.A.; Ekesi, S. Global risk of invasion by *Bactrocera zonata*: Implications on horticultural crop production under changing climatic conditions. *PLoS ONE* **2020**, *15*, e0243047.
52. Singh, K.; McClean, C.J.; Büker, P.; Hartley, S.E.; Hill, J.K. Mapping regional risks from climate change for rainfed rice cultivation in India. *Agric. Syst.* **2017**, *156*, 76–84. [[CrossRef](#)] [[PubMed](#)]

53. Papier, C.M.; Poulos, H.M.; Kusch, A. Invasive species and carbon flux: The case of invasive beavers (*Castor canadensis*) in riparian Nothofagus forests of Tierra del Fuego, Chile. *Clim. Chang.* **2019**, *153*, 219–234. [[CrossRef](#)]
54. Phillips, S.J.; Dudík, M. Modeling of species distributions with MaxEnt: New extensions and a comprehensive evaluation. *Ecography* **2008**, *31*, 161–175. [[CrossRef](#)]
55. Fielding, A.H.; Bell, J.F. A review of methods for the assessment of prediction errors in conservation presence/absence models. *Environ. Conserv.* **1997**, *24*, 38–49. [[CrossRef](#)]
56. Swets, J.A. Measuring the accuracy of diagnostic systems. *Science* **1988**, *240*, 1285–1293. [[CrossRef](#)] [[PubMed](#)]
57. Allouche, O.; Tsoar, A.; Kadmon, R. Assessing the accuracy of species distribution models: Prevalence, kappa and the true skill statistic (TSS). *J. Appl. Ecol.* **2006**, *43*, 1223–1232. [[CrossRef](#)]
58. Manning, M. The treatment of uncertainties in the fourth IPCC assignment report. *Adv. Clim. Chang. Res.* **2006**, *2*, 13–21.
59. O'Neill, B.C.; Tebaldi, C.; van Vuuren, D.P.; Eyring, V.; Friedlingstein, P.; Hurtt, G.; Knutti, R.; Kriegler, E.; Lamarque, J.F.; Lowe, J.; et al. The Scenario Model Intercomparison Project (ScenarioMIP) for CMIP6. *Geosci. Model Dev.* **2016**, *9*, 3461–3482. [[CrossRef](#)]
60. Zhang, L.X.; Chen, X.L.; Xin, X.G. Short commentary on CMIP6 Scenario Model Intercomparison Project (ScenarioMIP). *Clim. Chang. Res.* **2019**, *15*, 519–525.
61. Sillero, N. What does ecological modelling model? A proposed classification of ecological niche models based on their underlying methods. *Ecol. Model.* **2011**, *222*, 1343–1346. [[CrossRef](#)]
62. R Core Team. *R: A Language and Environment for Statistical Computing*; R Foundation for Statistical Computing: Vienna, Austria, 2018.
63. Castellarin, S.D.; Pfeiffer, A.; Sivilotti, P.; Degan, M.; Peterlunger, E.; Di Gaspero, G. Transcriptional regulation of anthocyanin biosynthesis in ripening fruits of grapevine under seasonal water deficit. *Plant Cell Environ.* **2007**, *30*, 1381–1399. [[CrossRef](#)] [[PubMed](#)]
64. Jiang, L.L.; Wang, J.; Zhang, X.Y.; Chen, R.W.; Hu, H.Y. Rainfall effect of rainfall on the quality of wine grape during the ripening stage at the east foot of Helan Mountain. *Chin. J. Agrometeorol.* **2020**, *41*, 156–161.
65. Sun, Z.X.; Bai, H.Q.; Ye, H.C.; Zhuo, Z.Q.; Huang, W.J. Three-dimensional modelling of soil organic carbon density and carbon sequestration potential estimation in a dryland farming region of China. *J. Geogr. Sci.* **2021**, *31*, 1453–1468. [[CrossRef](#)]
66. Cheng, G.; He, Y.N.; Yue, T.X.; Wang, J.; Zhang, Z.W. Effects of climatic conditions and soil properties on Cabernet Sauvignon berry growth and anthocyanin profiles. *Molecules* **2014**, *19*, 13683–13703. [[CrossRef](#)] [[PubMed](#)]
67. Wang, X.; Wang, H.; Li, H. The influence of recent climate variability on viticultural zoning and variety regionalisation of *Vitis vinifera* in China. *OENO One* **2020**, *54*, 523–541. [[CrossRef](#)]
68. Nesbitt, A.; Dorling, S.; Lovett, A. A suitability model for viticulture in England and Wales: Opportunities for investment, sector growth and increased climate resilience. *J. Land Use Sci.* **2018**, *13*, 414–438. [[CrossRef](#)]
69. Roy, P.; Grenier, P.; Barriault, E.; Logan, T.; Blondlot, A.; Bourgeois, G.; Chaumont, D. Probabilistic climate change scenarios for viticultural potential in Québec. *Clim. Chang.* **2017**, *143*, 43–58. [[CrossRef](#)]
70. Lereboullet, A.L.; Beltrando, G.; Bardsley, D.K.; Rouvellac, E. The viticultural system and climate change: Coping with long-term trends in temperature and rainfall in Roussillon, France. *Reg. Environ. Chang.* **2014**, *14*, 1951–1966. [[CrossRef](#)]
71. Dunn, M.; Rounsevell, M.D.A.; Boberg, F.; Clarke, E.; Christensen, J.; Madsen, M.S. The future potential for wine production in Scotland under high-end climate change. *Reg. Environ. Chang.* **2019**, *19*, 723–732. [[CrossRef](#)]
72. Lorenzo, M.; Ramos, A.M.; Brands, S. Present and future climate conditions for winegrowing in Spain. *Reg. Environ. Chang.* **2016**, *16*, 617–627. [[CrossRef](#)]
73. Lesk, C.; Rowhani, P.; Ramankutty, N. Influence of extreme weather disasters on global crop production. *Nature* **2016**, *529*, 84–87. [[CrossRef](#)] [[PubMed](#)]